Journal of Cellular Biotechnology 2 (2016/2017) 125–130
DOI 10.3233/JCB-15032
IOS Press

Characterization of benign periablational enhancement following multipolar radiofrequency ablation using perfusion CT in an *in-vivo* porcine liver model

Janis L. Vahldiek[a,*], Stefan F. Thieme[a], Ole Gemeinhardt[b], Franz Poch[b], Bernhard Hiebl[c], Kai S. Lehmann[b], B. Hamm[a] and Stefan M. Niehues[a]

[a]*Department of Radiology, Charité - University Medicine Berlin, Berlin, Germany*
[b]*Department of Surgery, Charité - University Medicine Berlin, Berlin, Germany*
[c]*Center for Medical Basic Research, Martin-Luther-University Halle-Wittenberg, Halle (Saale), Germany*

Abstract.
PURPOSE: Thermal ablation is an important interventional option in the management of liver tumors. Immediate postablational imaging regularly shows periablational enhancement. This peripheral hyperperfusion may induce heat-sink effects which could contribute to incomplete tumor ablation. To reduce the effect of hyperperfusion the feeding vessels source must be known. The aim of this study was to dynamically characterize the type of blood supply of the periablational enhancement zone immediately after hepatic radiofrequency ablation (RFA) using perfusion CT.
METHODS: We used an *in-vivo* porcine liver model. Multipolar RFA was performed in healthy pig livers. Immediate postablational perfusion CT was acquired. The contrast enhancement over time of the peripheral ablation zone, the aorta and the portal vein were recorded. Time differences of the peak periablational enhancement to the peak arterial perfusion and to the peak portalvenous perfusion were calculated and analyzed.
RESULTS: The perfusion peak of the periablational enhancement zone always occurred in mean 8.1 s after the arterial peak in the aorta and in mean 16.9 s before the peak in the portal vein.
CONCLUSIONS: Benign periablational enhancement is a result of primary arterial and not portalvenous hyperperfusion. In order to reduce heat sink effects, peri-ablational arterial balloon occlusion or transarterial chemoembolization may be beneficial during RFA.

Keywords: Ablation techniques, CT-perfusion, liver, animal investigations

1. Introduction

Radiofrequency ablation (RFA) is an important and minimal-invasive treatment option for hepatic tumors and metastases [1–7]. It belongs to the energy-based ablation modalities and relies on proper needle electrode placement into the tumor via an open, laparoscopic or percutaneous approach. The electrode delivers a high frequency alternating current into the surrounding tissue resulting in tissue heating. As tissue temperature exceeds 55°C, cell death occurs leading to coagulation necrosis

*Corresponding author: Dr. med. Janis Lucas Vahldiek, Charité, - Universitätsmedizin Berlin, Campus Benjamin Franklin - Klinik für Radiologie, Hindenburgdamm 30, 12203 Berlin, Germany. Tel.: +49 30 8445 3041; Fax: +49 30 450 7 527 953; E-mail: janis.vahldiek@charite.de.

surrounding the probe. The intended ablation zone should include the entire tumor volume including a safety margin of 5 to 10 mm to ensure complete ablation.

Benign periablational enhancement (BPE) can be visualized immediately after thermal ablation as hyperemic rim surrounding the ablated tissue on CT or MRI follow-up imaging [8]. Pathologic examinations showed that BPE is an inflammatory response to thermal ablation with initial reactive hyperaemia and subsequent fibrosis/giant cell reaction [9]. This induced hyperaemia may physically cause significant heat sink effects in the proximity of the ablation zone may limiting the final extent of the thermal destruction.

Heat sink effects are a major problem in thermal ablation procedures as they can cause incomplete tumor ablation and thus limit curative treatment approaches. They are also accused to account for the high post-ablation recurrence rates reported of up to 36.5 percent [4, 10–14].

Hepatic RFA has been successfully combined with arterial and portal-venous blood flow reduction/interruption resulting in improved patient survival and reduced tumor recurrence [15–17].

Data on the type of blood supply of the benign periablational enhancement zone, whether it is an arterial, portal-venous or mixed supply, is insufficient. Therefore, the aim of this study was to dynamically characterize the type of blood supply of the periablational enhancement zone immediately after hepatic radiofrequency ablation (RFA) using continuous CT-perfusion imaging.

2. Materials and methods

We utilized an *in-vivo* porcine liver model - a detailed description of the applied experimental setup has previously been published [18]. All principles of laboratory animal care according to the guidelines of the European Societies of Laboratory Animal Sciences were followed throughout the entire experiments. The regional office for health and social welfare approved the study.

2.1. In-vivo porcine liver model

The study was performed in 5 healthy domestic pigs aged 148 ± 16 days with an average body weight of $69\,\text{kg} \pm 2\,\text{kg}$. Intrahepatic multipolar RFA was performed using an open approach under general anesthesia. Three internally cooled bipolar electrodes (CelonProSurge 150-T30, Olympus Surgical Technologies Europe, Hamburg, Germany) and a corresponding generator (CelonPower System, Olympus Winter & Ibe GmbH, Teltow, Germany) were utilized. The probes were introduced into the liver strictly parallel with a constant distance of 15 mm or 20 mm using CT-guidance. Every lesion in this study was ablated with a power of 90 W and a target energy application of 50 kJ. The probe's tips were placed centrally in one of the four liver lobes. Every ablation was performed during physiological liver perfusion.

2.2. Perfusion CT

Immediately after every RF-ablation, perfusion CT (pCT) of the liver was acquired. We used an 80-slice MDCT scanner (Aquilion PRIME, Toshiba Medical Systems, Otawara, Japan) and the following CT parameters: 100 kV, 200 mA, 0.35 s rotation time, mean mAs = 108. Before acquisition, 40 ml of Iomeprol in a concentration of 400 mg/ml were automatically injected with an injection speed of 5 ml/s (Imeron® 400, Bracco Imaging, Milan, Italy). In total, a post-ablation pCT consisted of 40 single and consecutive scans following a standardized time protocol. Shuttle mode for constant bidirectional CT table movement was used to cover a craniocaudal length of 16 cm.

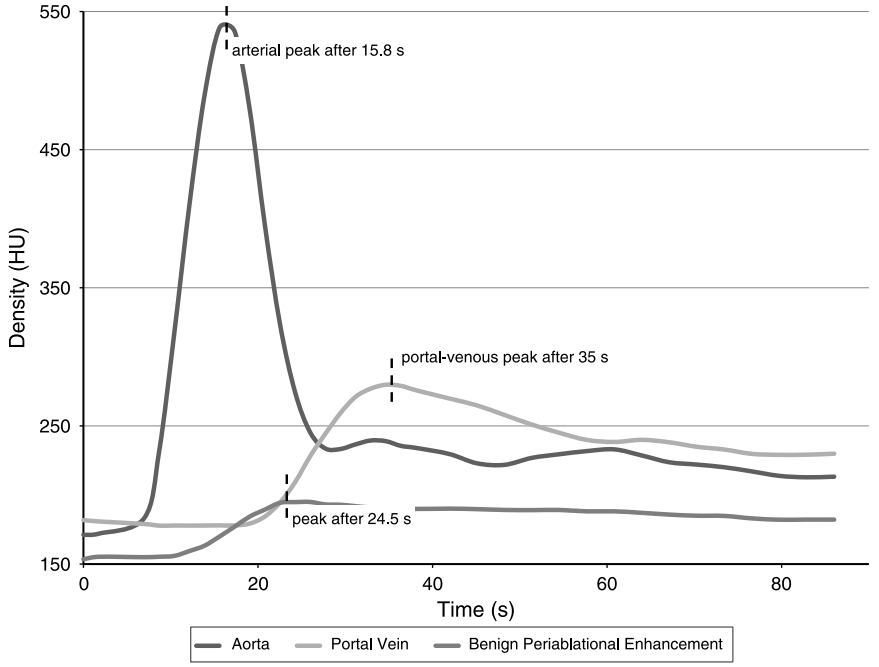

Fig. 1. Exemplary time-density-curve for one single ablation zone: The peak of the benign periablational enhancement occurred 8.7 seconds after the peak perfusion in the abdominal aorta and 10.5 seconds before the peak perfusion in the central portal vein.

2.3. Evaluation and analysis

The acquired pCT datasets were loaded into the 4D CT Body Perfusion tool of the Vitrea®-Software (Vital Images, Minnetonka, USA). In order to generate time-density-curves of the arterial and the portal-venous perfusion, circular ROIs were drawn in the abdominal aorta and in the central portal vein. A freehand ROI encompassing the complete benign periablational enhancement zone surrounding a single ablation zone was drawn to generate a time-density-curve of the ablation's rim perfusion. Time to peak perfusion of all three resulting curves was recorded in order to calculate the time interval between arterial and BPE-peak as well as the interval between portal-venous and BPE-peak (Fig. 1). Furthermore, the maximum diameter of the periablational enhancement zone in each ablation was documented.

SPSS was used for data analysis (IBM Corp. Released 2013. IBM SPSS Statistics for Macintosh, Version 22.0. Armonk, NY: IBM Corp.). Descriptive statistical analysis included the calculation of mean values and corresponding standard deviations.

3. Results

We conducted ten RF-ablations in 5 animals. Benign periablational enhancement could be detected in eight ablations on immediate post-ablation pCT as hyperdense and circular rim surrounding the hypodense ablation zone (Fig. 2). The remaining two ablations showed diffuse intra-lesional hemorrhage on pCT from that a periablational enhancement zone could not explicitly be differentiated. Thus, these two lesions were excluded from further analysis.

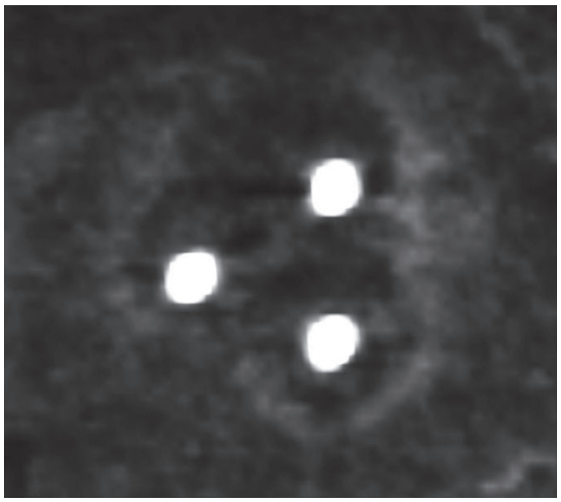

Fig. 2. Immediate post-ablation perfusion CT shows the benign periablational enhancement surrounding the hypodense ablation zone.

Benign periablational enhancement rim showed a mean maximum diameter of 4.3 ± 0.9 mm ($n = 8$ ablations). Figure 1 exemplarily depicts a time-density-curve for one ablation zone. In all eight ablations, the generated time-density-curves showed that benign periablational enhancement could be visualized after arterial perfusion and before portal-venous perfusion started. After intravenous contrast injection, the peak aortal density was observed after 18.7 ± 5.3 s (mean $\pm$ standard deviation), the peak BPE density after 26.8 ± 5.0 s and the peak portal density after 43.7 ± 8.0 s (N = 8). The peak of the benign periablational enhancement arose in mean 8.1 ± 1.6 s after the peak perfusion in the abdominal aorta and 16.9 ± 5.5 s before the peak perfusion in the central portal vein. We did not observe any ablation zone that showed peak perfusion of the periablational enhancement zone after portal-venous perfusion.

4. Discussion

The applied study design allowed for the investigation of the benign periablational enhancement's type of blood supply using immediate postablational perfusion CT. Our results suggest an arterial and not a portalvenous hyperperfusion of the periablational rim following multipolar RFA of the liver.

Benign peripheral enhancement can be visualized on contrast-enhanced ultrasonographic, CT- or MR-imaging immediately after thermal ablation procedures such as RFA, laser ablation and microwave ablation [9]. It is caused by vasodilation in the context of an instant inflammatory response to thermal damage resulting in reactive hyperaemia [8, 19]. This reaction can raise significant heat sink effects in the proximity of the ablation zone already during thermal ablation, although this hypothesis has never been proven and is certainly hard to verify. Peri-procedural heat sink effects are blamed for the high local recurrence rates after thermal ablation procedures [12–14, 20, 21]. To avoid or reduce these heat sink effects thermal ablation procedures have been successfully combined with transcatheter arterial chemoembolization and selective balloon occlusion of hepatic vessels [15–17, 22, 23]. Our results support the approach of temporarily interrupting the arterial blood flow during thermal procedures of the liver in order to avoid reduced heat distribution in the proximity of the targeted tumor volume.

This study has certain limitations. Although the results of this study were performed using a porcine liver model, we think that our results can be transferred to humans, since porcine animal models

have broadly and successfully been used in translational research [24–26]. The use of intravenous agents for general anesthesia denotes a further limitation of this study as they may have altered hepatic perfusion parameters. We used ketamine and xylazine for general anesthesia. Both agents are widely used in animal experiments and have proven to marginally influence hepatic perfusion and metabolism [27–29].

In conclusion, benign periablational enhancement after RFA is a result of arterial and not portal-venous hyperperfusion. It is a potential source of periablational cooling effects that could lead to incomplete tumor ablation, early relapse and limitations in achievable lesion size. Thus, interrupting the arterial blood flow using balloon occlusion or transarterial chemoembolization during RFA is a promising approach in order to reduce heat sink effects especially in the boundary area when ablating larger tumor volumes.

References

[1] Sartori S, Tombesi P, Macario F, et al. Subcapsular liver tumors treated with percutaneous radiofrequency ablation: A prospective comparison with nonsubcapsular liver tumors for safety and effectiveness. Radiology 2008;248:670-79.
[2] Tanabe KK, Curley SA, Dodd GD, Siperstein AE, Goldberg SN. Radiofrequency ablation: The experts weigh in. Cancer 2004;100:641-50.
[3] Amersi FF, McElrath-Garza A, Ahmad A, et al. Long-term survival after radiofrequency ablation of complex unresectable liver tumors. Arch Surg 2006;141:581-7; discussion 587-588.
[4] Hildebrand P, Kleemann M, Roblick UJ, et al. Radiofrequency-ablation of unresectable primary and secondary liver tumors: Results in 88 patients. Langenbecks Arch Surg 2006;391:118-23.
[5] Stang A, Fischbach R, Teichmann W, Bokemeyer C, Braumann D. A systematic review on the clinical benefit and role of radiofrequency ablation as treatment of colorectal liver metastases. Eur J Cancer 2009;45:1748-56.
[6] Tatli S, Tapan U, Morrison PR, Silverman SG. Radiofrequency ablation: Technique and clinical applications. Diagn Interv Radiol 2012;18:508-16.
[7] Rathke H, Hamm B, Guttler F, et al. Comparison of four radiofrequency ablation systems at two target volumes in an ex vivo bovine liver model. Diagn Interv Radiol 2014;20:251-8.
[8] Wu H, Patel RB, Zheng Y, et al. Differentiation of benign periablational enhancement from residual tumor following radio-frequency ablation using contrast-enhanced ultrasonography in a rat subcutaneous colon cancer model. Ultrasound Med Biol 2012;38:443-53.
[9] Goldberg SN, Grassi CJ, Cardella JF, et al. Image-guided tumor ablation: Standardization of terminology and reporting criteria. Radiology 2005;235:728-39.
[10] Snoeren N, Nijkamp MW, Berendsen T, et al. Multipolar radiofrequency ablation for colorectal liver metastases close to major hepatic vessels. Surgeon 2015;13:77-82.
[11] Welp C, Siebers S, Ermert H, Werner J. Investigation of the influence of blood flow rate on large vessel cooling in hepatic radiofrequency ablation. Biomed Tech (Berl) 2006;51:337-46.
[12] Frericks BB, Ritz JP, Albrecht T, et al. Influence of intrahepatic vessels on volume and shape of percutaneous thermal ablation zones: In vivo evaluation in a porcine model. Invest Radiol 2008;43:211-18.
[13] Khan MR, Poon RT, Ng KK, et al. Comparison of percutaneous and surgical approaches for radiofrequency ablation of small and medium hepatocellular carcinoma. Arch Surg 2007;142:1136-43; discussion 1143.
[14] Mulier S, Ni Y, Jamart J, Ruers T, Marchal G, Michel L. Local recurrence after hepatic radiofrequency coagulation: Multivariate meta-analysis and review of contributing factors. Ann Surg 2005;242:158-71.
[15] Iezzi R, Cesario V, Siciliani L, et al. Single-step multimodal locoregional treatment for unresectable hepatocellular carcinoma: Balloon-occluded percutaneous radiofrequency thermal ablation (BO-RFA) plus transcatheter arterial chemoembolization (TACE). Radiol Med 2013;118:555-69.
[16] Subrt Z, Ferko A, Hoffmann P, et al. Temporary liver blood-outflow occlusion increases effectiveness of radiofrequency ablation: An experimental study on pigs. Eur J Surg Oncol 2008;34:346-52.
[17] Yi Y, Zhang Y, Wei Q, et al. Radiofrequency ablation or microwave ablation combined with transcatheter arterial chemoembolization in treatment of hepatocellular carcinoma by comparing with radiofrequency ablation alone. Chin J Cancer Res 2014;26:112-8.
[18] Vahldiek JL, Lehmann KS, Poch F, et al. Measuring and optimizing results in multipolar RFA: Techniques and early findings in an experimental setting. Clin Hemorheol Microcirc 2014;58:77-87.

[19] Emami B, Nussbaum GH, TenHaken RK, Hughes WL. Physiological effects of hyperthermia: Response of capillary blood flow and structure to local tumor heating. Radiology 1980;137:805-9.
[20] Kuvshinoff BW, Ota DM. Radiofrequency ablation of liver tumors: Influence of technique and tumor size. Surgery 2002;132:605-11; discussion 611-602.
[21] Thanos L, Mylona S, Galani P, Pomoni M, Pomoni A, Koskinas I. Overcoming the heat-sink phenomenon: Successful radiofrequency thermal ablation of liver tumors in contact with blood vessels. Diagn Interv Radiol 2008;14:51-6.
[22] Liu HC, Shan EB, Zhou L, et al. Combination of percutaneous radiofrequency ablation with transarterial chemoembolization for hepatocellular carcinoma: Observation of clinical effects. Chin J Cancer Res 2014;26:471-7.
[23] Peng ZW, Zhang YJ, Chen MS, et al. Radiofrequency ablation with or without transcatheter arterial chemoembolization in the treatment of hepatocellular carcinoma: A prospective randomized trial. J Clin Oncol 2013;31:426-32.
[24] Kobayashi E, Hishikawa S, Teratani T, Lefor AT. The pig as a model for translational research: Overview of porcine animal models at Jichi Medical University. Transplant Res 2012;1:8.
[25] Lee KC, Palacios Jimenez C, Alibhai H, et al. A reproducible, clinically relevant, intensively managed, pig model of acute liver failure for testing of therapies aimed to prolong survival. Liver Int 2013;33:544-51.
[26] Swindle MM, Makin A, Herron AJ, Clubb FJ Jr, Frazier KS. Swine as models in biomedical research and toxicology testing. Vet Pathol 2012;49:344-56.
[27] Chaib S, Charrueau C, Neveux N, Coudray-Lucas C, Cynober L, De Bandt AP. Isolated perfused liver model: The rat and guinea pig compared. Nutrition 2004;20:458-64.
[28] Green CJ, Knight J, Precious S, Simpkin S. Ketamine alone and combined with diazepam or xylazine in laboratory animals: A 10 year experience. Lab Anim 1981;15:163-70.
[29] He S, Atkinson C, Qiao F, Chen X, Tomlinson S. Ketamine-xylazine-acepromazine compared with isoflurane for anesthesia during liver transplantation in rodents. J Am Assoc Lab Anim Sci 2010;49:45-51.